Refined critical balance in strong Alfvénic turbulence

Alfred Mallet (University of New Hampshire), Alexander A. Schekochihin (University of Oxford), Benjamin D. G. Chandran (University of New Hampshire)

1. Introduction

We study the statistics of turbulence in a numerical simulation of the RMHD equations, which describe strong Alfvénic turbulence:

$$\partial_t \mathbf{z}_\perp^\pm \mp v_A \partial_z \mathbf{z}_\perp^\pm + \mathbf{z}_\perp^\mp \cdot \nabla_\perp \mathbf{z}_\perp^\pm = -\nabla_\perp p, \tag{1}$$

The critical balance conjecture [5] states that the chararacteristic nonlinear $\tau_{\rm nl}$ and linear $\tau_{\rm A}$ times, defined as

$$\tau_{\rm nl}^\pm \doteq \frac{\lambda}{\delta z_\perp^\mp \sin\theta}, \quad \tau_{\rm A}^\pm \doteq \frac{l_\parallel^\pm}{v_A}, \tag{2}$$

are comparable at each scale. *We present numerical evidence that in strong Alfvénic turbulence, the critical balance principle is scale invariant,* in the sense that *the probability distribution of the ratio of these times, $\chi^\pm \doteq \tau_{\rm A}^\pm/\tau_{\rm nl}^\pm$ is independent of scale.* This result only holds if the local alignment of the Elsasser fields is taken into account in calculating the nonlinear time.

The scale-invariance of critical balance (while all other quantities of interest are strongly intermittent, i.e., have scale-dependent distributions) suggests that it is the most robust of the scaling principles used to describe Alfvénic turbulence.

We examine the joint statistical distribution of $\delta z_\perp^\pm$, $l_\parallel^\pm$ and θ as a function of λ using data from a 1024^3 numerical simulation, described in detail in [6], and thus we may construct the distributions of $\tau_{\rm A}^\pm$, $\tau_{\rm nl}^\pm$ and $\chi^\pm$.

2. Definitions

The fluctuation amplitudes are measured in terms of increments

$$\delta z_\perp^\pm \doteq |\delta \mathbf{z}_\perp^\pm| \doteq |\mathbf{z}_\perp^\pm(\mathbf{r}_0+\mathbf{r}_\perp) - \mathbf{z}_\perp^\pm(\mathbf{r}_0)|, \quad \lambda \doteq |\mathbf{r}_\perp|, \tag{3}$$

where $\mathbf{r}_0$ is an arbitrary point and $\mathbf{r}_\perp$ the separation in the plane perpendicular to $\mathbf{B}_0$. The alignment angle is given by

$$\sin\theta \doteq \frac{|\delta \mathbf{z}_\perp^+ \times \delta \mathbf{z}_\perp^-|}{\delta z_\perp^+ \delta z_\perp^-}. \tag{4}$$

The parallel coherence length $l_\parallel^\pm$ corresponding to a perpendicular separation $\mathbf{r}_\perp$ is defined as the distance along the *perturbed* field line at which the Elsasser-field increment is the same as $\delta z_\perp^\pm$ [4, 7, 8]:

$$\left|\mathbf{z}_\perp^\pm\left(\mathbf{r}_0 + (\mathbf{r}_\perp + l_\parallel^\pm \hat{\mathbf{b}}_{\rm loc})/2\right) - \mathbf{z}_\perp^\pm\left(\mathbf{r}_0 + (\mathbf{r}_\perp - l_\parallel^\pm \hat{\mathbf{b}}_{\rm loc})/2\right)\right| = |\mathbf{z}_\perp^\pm(\mathbf{r}_0+\mathbf{r}_\perp) - \mathbf{z}_\perp^\pm(\mathbf{r}_0)|,$$

where $\hat{\mathbf{b}}_{\rm loc} = \mathbf{B}_{\rm loc}/|\mathbf{B}_{\rm loc}|$ is the unit vector along the "local mean field" $\mathbf{B}_{\rm loc} \doteq \mathbf{B}_0 + [\mathbf{b}_\perp(\mathbf{r}_0) + \mathbf{b}_\perp(\mathbf{r}_0+\mathbf{r}_\perp)]/2$.

At each scale λ, the joint probability distribution fuction (PDF) $P(\delta z_\perp^+, \delta z_\perp^-, \theta, l_\parallel^+, l_\parallel^-|\lambda)$ contains all the information one customarily requires to characterize the structure of Alfvénic turbulence.

3. Intermittency

A standard question of all turbulence studies is how the increments $\delta z_\perp^+$ depend on λ. *The distribution of $\delta z_\perp^+$ is clearly not scale-invariant,* as is made manifest by Fig. 1, where we show $P(\delta z_\perp^+|\lambda)$ rescaled to $\overline{\delta z}_\perp^+$ at each λ.

The salient feature of this PDF is that it broadens at smaller λ — a classic case of intermittency understood as scale dependence of the distribution's shape. This broadening may be consistent with a lognormal [9] or a log-Poisson [3] distribution.

Equivalently, the scaling of $\delta z_\perp^+$ depends on which moment of this distribution one uses. Fig. 1 (inset) shows the scalings of the rms increment $S_2^{1/2}(\lambda) \doteq \langle(\delta z_\perp^+)^2|\lambda\rangle^{1/2}$, the geometric mean $\overline{\delta z}_\perp^+ \doteq \exp\langle \ln \delta z_\perp^+|\lambda\rangle$, and the 4th-order increment, $S_4^{1/4}(\lambda) \doteq \langle(\delta z_\perp^+)^4|\lambda\rangle^{1/4}$.

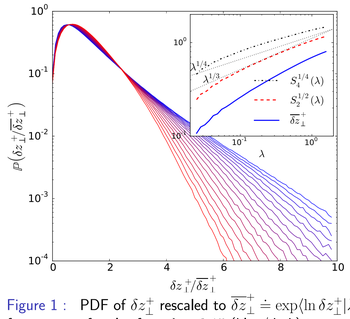

Figure 1 : PDF of $\delta z_\perp^+$ rescaled to $\overline{\delta z}_\perp^+ \doteq \exp\langle \ln \delta z_\perp^+|\lambda\rangle$, for a range of scales from $\lambda = 0.15$ (blue/dark) to $\lambda = 0.80$ (red/light). *Inset:* the rms (2nd-order) increment $S_2^{1/2}(\lambda) \doteq \langle(\delta z_\perp^+)^2|\lambda\rangle^{1/2}$ (red dashed line), the 4th-order increment, $S_4^{1/4}(\lambda) \doteq \langle(\delta z_\perp^+)^4|\lambda\rangle^{1/4}$ (black dash-dotted line), and the "typical" increment $\overline{\delta z}_\perp^+$ (blue solid line); the slopes $\lambda^{1/4}$ (Boldyrev [2]) and $\lambda^{1/3}$ (Goldreich–Sridhar [5]) are given for reference; all increments are normalized to the overall rms fluctuation level.

4. Characteristic times

The distribution of $\tau_{\rm A}^\pm = l_\parallel^\pm/v_A$ is simply the distribution of the parallel coherence length. Its geometric mean is shown in Fig. 2(a, inset) and scales like $\overline{\tau}_{\rm A}^+ \doteq \exp\langle \ln \tau_{\rm A}^+\rangle \propto \lambda^{1/2}$, consistent with [2].

The PDFs of the rescaled quantity $\tau_{\rm A}^+/\lambda^{1/2}$ for a range of λ are shown in Fig. 2(a): at smaller $\tau_{\rm A}^+/\lambda^{1/2}$ there is a scale-invariant collapse, but at larger values, the PDF becomes non-scale-invariant — with a systematically shallower tail at larger λ.

The geometric mean of the nonlinear time is shown in Fig. 2(b, inset) and, like $\overline{\tau}_{\rm A}^+$, scales as $\overline{\tau}_{\rm nl}^+ \doteq \exp\langle \ln \tau_{\rm nl}^+|\lambda\rangle \propto \lambda^{1/2}$.

The PDFs of the rescaled inverse nonlinear time, $\lambda^{1/2}/\tau_{\rm nl}^+$, are shown in Fig. 2(b). There is a scale-invariant collapse at small values of the rescaled quantity (i.e., relatively longer $\tau_{\rm nl}$), and a non-scale-invariant tail at larger values, systematically shallower at smaller λ.

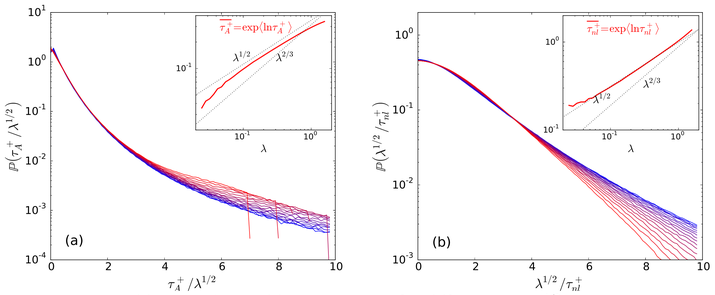

Figure 2 : PDFs of (a) $\tau_{\rm A}^+ \doteq l_\parallel^+/v_A$ and (b) the inverse of $\tau_{\rm nl}^+$ [Eq. (2)], rescaled by $\lambda^{1/2}$, for a range of scales from from $\lambda = 0.15$ (blue/dark) to $\lambda = 0.80$ (red/large). *Insets:* "Typical times" (a) $\overline{\tau}_{\rm A} \doteq \exp\langle \ln \tau_{\rm A}^+\rangle$ and (b) $\overline{\tau}_{\rm nl} \doteq \exp\langle \ln \tau_{\rm nl}^+\rangle$ vs. λ with $\lambda^{1/2}$ and $\lambda^{2/3}$ scalings shown for reference.

5. Refined critical balance

The behaviour of the distribution of the nonlinear time fits neatly with that of the distribution of the Alfvén time. The cores of both distributions (roughly, $\tau_{\rm A}^+/\lambda^{1/2} \lesssim 3$ and $\lambda^{1/2}/\tau_{\rm nl}^+ \lesssim 3$ in Fig. 2) are scale invariant. On the other hand, their tails vary with λ in opposite senses, with the tail of $\tau_{\rm A}^\pm/\lambda^{1/2}$ ($\lambda^{1/2}/\tau_{\rm nl}^\pm$) becoming steeper (shallower) as λ decreases. Because of this, the distribution of their product $\chi^\pm$, defined as

$$\chi^\pm \doteq \frac{\tau_{\rm A}^\pm}{\tau_{\rm nl}^\pm} = \frac{l_\parallel^\pm \delta z_\perp^\mp \sin\theta}{v_A \lambda}, \tag{5}$$

does not change at all: *$P(\chi^+|\lambda)$, shown in Fig. 3, is independent of λ across the inertial range and all its moments are constant:* e.g., $\langle\chi^+|\lambda\rangle$ is shown in the inset of Fig. 3 (alongside it, we show the mean nonlinearity parameter without the $\sin\theta$ factor, $\langle\chi^+/\sin\theta|\lambda\rangle$; it is not scale-independent, which emphasizes that alignment is an essential ingredient of the RCB).

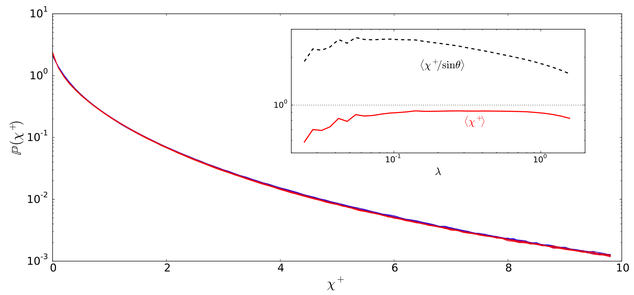

Figure 3 : PDF of χ^+ (defined by Eq. (5)) for a range of scales from $\lambda = 0.15$ (blue/dark) to $\lambda = 0.80$ (red/large). Data collapse is nearly perfect. *Inset:* the mean nonlinearity parameter $\langle\chi^+\rangle$ vs. λ (red/solid) and the same without account for alignment, $\langle\chi^+/\sin\theta\rangle$ (black/dashed).

6. Alignment

At every scale λ, the fluctuation amplitude $\delta z_\perp^\mp$ and the alignment angle θ turn out to be anticorrelated (cf. [1]). This is evident in the conditional PDF $P(\sin\theta|\delta z_\perp^+/\overline{\delta z}_\perp^+, \lambda)$, shown in Fig. 4. Fluctuations whose amplitudes are large relative to the "typical" value $\overline{\delta z}_\perp^+$ tend to be well aligned, whereas the weaker fluctuations ($\delta z_\perp^+/\overline{\delta z}_\perp^+ \lesssim 1$) are unaligned. The alignment of the stronger fluctuations appears to get statistically "tighter" at smaller scales. Thus, for the stronger fluctuations, the nonlinear interaction is reduced by alignment more than for the weaker ones.

The anticorrelation between alignment and amplitude is somewhat at odds with Boldyrev's interpretation of the alignment angle as determined by the angular wander within any given fluctuation ($\theta \sim \delta b_\perp/B_0$), but rather *suggests that alignment is caused by dynamical shearing of a weaker Elsasser field by a stronger one [3].*

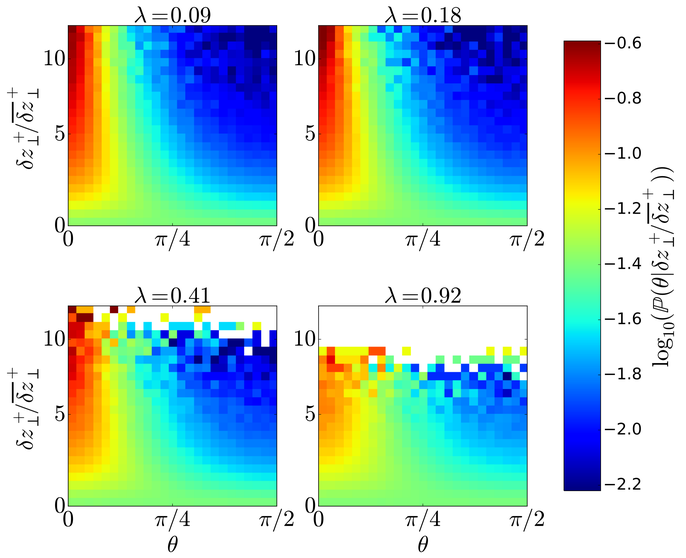

Figure 4 : PDF of the alignment angle θ conditional on the fluctuation amplitude $\delta z_\perp^+$ relative to "typical" value $\overline{\delta z}_\perp^+ \doteq \exp\langle \ln \delta z_\perp^+|\lambda\rangle$, viz., $P(\sin\theta|\delta z_\perp^+/\overline{\delta z}_\perp^+, \lambda)$, plotted for four representative scales λ (as shown).

7. Conclusion

The results presented above imply that the structure of Alfvénic turbulence is set by two fundamental effects: establishment of a critical balance, *which occurs in a scale-invariant fashion* (probably due to the upper limit on the parallel coherence length of turbulent fluctuations imposed by causality over a nonlinear decorrelation time), and systematic alignment of the higher-amplitude fluctuations (probably due to dynamical mutual shearing of Elsasser fields). The first of these results suggests that critical balance — quantitatively amounting, as we have argued, to the RCB conjecture — is perhaps the most robust and reliable of the physical principles undepinning scaling theories of Alfvénic turbulence.

References

[1] A. Beresnyak and A. Lazarian, Astrophys. J. **640** (2006), L175.

[2] S. Boldyrev, Phys. Rev. Lett. **96** (2006), 115002.

[3] B. D. G. Chandran, A. A. Schekochihin, and A. Mallet, arXiv:1403.6354 (2014).

[4] J. Cho and E. T. Vishniac, Astrophys. J. **539** (2000), 273.

[5] P. Goldreich and S. Sridhar, Astrophys. J. **438** (1995), 763.

[6] A. Mallet, A. A. Schekochihin, and B. D. G. Chandran, MNRAS **449** (2015), L77–L81.

[7] J. Maron and P. Goldreich, Astrophys. J. **554** (2001), 1175.

[8] W. H. Matthaeus, S. Servidio, P. Dmitruk, V. Carbone, S. Oughton, M. Wan, and K. T. Osman, Astrophys. J. **750** (2012), 103.

[9] V. Zhdankin, S. Boldyrev, and J. Mason, Astrophys. J. Lett. **760** (2012), L22.